

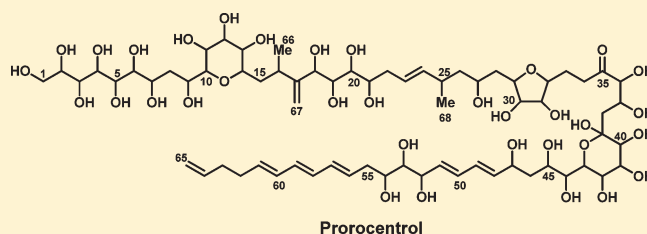
# Prorocentrol, a Polyoxy Linear Carbon Chain Compound Isolated from the Toxic Dinoflagellate *Prorocentrum hoffmannianum*

Kohtaro Sugahara, Yoshiaki Kitamura, Michio Murata,<sup>†</sup> Masayuki Satake,\* and Kazuo Tachibana\*

Department of Chemistry, School of Science, University of Tokyo, 7-3-1 Hongo, Bunkyo-ku, Tokyo 113-0033, Japan

**S** Supporting Information

**ABSTRACT:** A polyoxy linear carbon chain compound, prorocentrol (**1**), was isolated from cultured cells of the dinoflagellate *Prorocentrum hoffmannianum*, which produces a polyether carboxylic acid, okadaic acid. The structure of **1** was elucidated by detailed analyses of 2D NMR spectra. Compound **1** possesses 30 hydroxy groups, 1 ketone, and 8 double bonds on the C65-linear carbon chain. Its partial relative configuration was deduced by the proton–proton and long-range carbon–proton coupling constants, and compound **1** showed moderate cytotoxicity and antidiatom activity.



## INTRODUCTION

Marine dinoflagellates produce a variety of secondary metabolites possessing unique structural features and potent biological activities.<sup>1</sup> Among them, long linear carbon chain compounds having polyoxy functional groups are one of dominant classes of marine dinoflagellate products. Amphidinols,<sup>2</sup> luteophanols,<sup>3</sup> lingshuiols,<sup>4</sup> karatungols,<sup>5</sup> colopsinol,<sup>6</sup> and amphezonol<sup>7</sup> from *Amphidinium* spp., ostreocins from *Ostreopsis siamensis*,<sup>8</sup> durinskio A from *Durinskia* sp.,<sup>9</sup> symbiospirols from *Symbiodinium* sp.,<sup>10</sup> and karlotoxins from *Karlodinium veneficum*<sup>11</sup> are representative compounds in this class. Each of them has both a hydrophilic part consisting of polyhydroxy groups and a hydrophobic part with a polyene structure or an alkyl chain in the molecule. This amphiphilic nature must be important for expression of their specific bioactivities such as antifungal, cytotoxic, or hemolytic activities.<sup>12</sup>

The genus *Prorocentrum* also produces a variety of bioactive compounds, okadaic acid and its analogues,<sup>1</sup> prorocentrolides,<sup>13</sup> spiro-prorocentrimine,<sup>14</sup> hoffmanniolide,<sup>15</sup> and prorocentin.<sup>16</sup> These compounds have different skeletal features: polyether carboxylic acid, macrocyclic imine, lactone, and polyether alcohol. The okadaic acids are common secondary metabolites produced by *Prorocentrum* spp., whereas production of other compounds, e.g., prorocentrolides, spiro-prorocentrimine, hoffmanniolide, and prorocentin, are thought to depend on the nature of clones or species. These compounds except prorocentin were obtained from a butanol-soluble fraction of the algal extracts. Thus, *Prorocentrum* often produces intriguing butanol-soluble compounds in addition to the okadaic acids. Our continuous efforts for search of new bioactive compounds led to isolation of a polyoxy long linear carbon chain compound, prorocentrol (**1**), from the butanol-soluble fraction of *P. hoffmannianum* Faust (CCMP 683).<sup>17</sup>

To reveal the configuration of these natural products is a quite essential and challenging stage for further investigation of mode

of action and synthetic works. However, configurational analyses on these compounds especially in acyclic systems often face to problems, since they rarely form crystals suitable for X-ray analysis. In addition, a NOE-based method is inapplicable because of the multiple conformational exchanges. Against such unfavorable backgrounds in the conventional NMR method, Murata and co-workers established the *J*-based configurational analysis (JBCA),<sup>18</sup> which is a relative configurational determination method through conformational determination. The JBCA enabled us to distinguish between possible relative configurations even if conformational exchange occurs, since the coupling constants reflect the ratio of the conformers as weighted mean. To date, the JBCA has been applied for relative configurational analysis of natural products that possess many chiral centers on the acyclic chain such as amphidinol-3,<sup>19</sup> maitotoxin,<sup>20</sup> zooxanthellatoxin,<sup>18</sup> karlotoxin-2,<sup>21</sup> symbiopolyol,<sup>22</sup> belizeanolide,<sup>23</sup> several chlorosulfolipids from *Ochromonas danica*,<sup>24</sup> and versipelostatin.<sup>25</sup> Especially, the conformations of monensin<sup>26</sup> and okadaic acid<sup>27</sup> were analyzed in solution and compared with each of their crystalline structures. Therefore, the JBCA was applied for elucidation of the relative configuration of **1**. In this paper we report the isolation and structural determination including the partial relative configuration of **1**.

## RESULT AND DISCUSSION

Harvested cells by centrifugation were extracted with MeOH and then acetone for three times each and partitioned between hexane/H<sub>2</sub>O, EtOAc/H<sub>2</sub>O, and then BuOH/H<sub>2</sub>O. The BuOH layer was further partitioned between 0.15% aq AcOH and EtOAc for elimination of okadaic acid. The water-soluble fraction was chromatographed on an ODS column with 80% and 100% aq

**Received:** December 29, 2010

**Published:** March 22, 2011

Table 1.  $^1\text{H}$  and  $^{13}\text{C}$  NMR Data for **1** in Pyridine- $d_5$ /D $_2$ O (6:1)<sup>a</sup>

pos	$\delta_{\text{C}}$ , (mult)	$\delta_{\text{H}}$ , mult, J in Hz	pos	$\delta_{\text{C}}$ , (mult)	$\delta_{\text{H}}$ , mult, J in Hz	pos	$\delta_{\text{C}}$ , (mult)	$\delta_{\text{H}}$ , mult, J in Hz
1a	64.6, (t)	4.19, dd, 6.4, 11.1	25	33.5, (d)	2.56, br ddd, 4.1, 8.4, 6.6	47	70.3, (d)	4.72, br dd, 4.7, 9.9
1b		4.37, dd, 3.6, 11.1	26a	45.4, (t)	1.43, ddd, 8.7, 3.6, 14.1	48	136.9, (d)	5.86, dd, 5.9, 14.6
2	72.2, (d)	4.50, ddd, 3.6, 6.4, 8.2	26b		1.59, ddd, 4.7, 9.3, 14.6	49	129.3, (d)	6.38, dd, 10.9, 16.0
3	71.5, (d)	4.66, dd, 2.2, 8.2	27	66.5, (d)	4.14, dddd, 3.5, 8.8, 3.5, 8.8	50	130.3, (d)	6.52, dd, 15.1, 10.5
4	71.7, (d)	4.92, dd, 2.2, 6.8	28a	42.8, (t)	1.86, ddd, 3.5, 8.7, 13.5	51	135.4, (d)	6.17, dd, 6.4, 15.1
5	73.4, (d)	4.61, dd, 6.8, 7.3	28b		2.04, ddd, 9.2, 5.2, 14.0	52	72.0, (d)	5.00, dd, 6.4, 3.2
6	76.5, (d)	4.42, dd, 7.3, 4.5	29	78.3, (d)	4.52, ddd, 8.0, 4.5, 8.7	53	76.8, (d)	3.93, dd, 7.7, 2.9
7	73.0, (d)	4.81, ddd, 5.3, 8.2, 2.7	30	78.0, (d)	4.16, dd, 8.1, 4.3	54	71.6, (d)	4.33, ddd, 3.5, 7.6, 9.3
8a	36.2, (t)	2.18, ddd, 8.2, 8.7, 14.6	31	72.2, (d)	4.30, dd, 3.8, 2.5	55a	37.6, (t)	2.72, ddd, 7.6, 10.0, 15.5
8b		2.86, ddd, 2.3, 3.2, 14.1	32	79.8, (d)	4.11, dt, 2.5, 7.3	55b		2.96, ddd, 3.5, 7.6, 10.9
9	69.0, (d)	4.70, ddd, 3.2, 8.7, 9.1	33	23.9, (t)	2.32, br dd, 3.5, 7.0	56	132.6, (d)	6.14, ddd, 15.5, 6.7, 6.7
10	80.3, (d)	4.24, dd, 9.1, 2.7	34a	35.8, (t)	3.00, m	57	132.6, (d)	6.29, dd, 15.1, 10.1
11	68.8, (d)	4.94, dd, 2.7, 3.6	34b		3.15, m	58	132.2, (d)	6.17, dd, 14.2, 10.0
12	72.2, (d)	4.40, dd, 3.6, 8.2	35	213.0, (s)		59	131.0, (d)	6.09, dd, 10.0, 14.2
13	72.3, (d)	4.22, dd, 8.2, 8.0	36	80.8, (d)	4.57, d, 1.7	60	131.2, (d)	6.04, dd, 10.5, 13.7
14	75.4, (d)	4.09, ddd, 8.0, 4.2, 8.9	37	68.9, (d)	5.18, ddd, 1.7, 4.1, 9.1	61	133.3, (d)	5.60, dd, 14.6, 6.4
15a	40.1, (t)	1.91, ddd, 8.9, 4.5, 14.6	38a	41.6, (t)	2.54, dd, 2.2, 13.7	62	32.0, (t)	2.05, dt, 6.4, 14.1
15b		2.50, ddd, 5.3, 8.2, 14.6	38b		2.88, dd, 9.1, 15.1	63	33.3, (t)	2.01, dt, 6.0, 14.6
16	34.2, (d)	2.92, ddt, 5.9, 8.2, 6.6	39	100.9, (s)		64	138.1, (d)	5.73, ddt, 6.4, 10.5, 17.4
17	155.6, (s)		40	67.9, (d)	4.56, d, 2.9	65a	114.9, (t)	4.93, ddd, 0.9, 2.3, 10.5
18	74.1, (d)	4.88, d, 4.6	41	73.5, (d)	4.75, dd, 4.7, 2.9	65b		4.97, ddd, 1.0, 3.2, 17.4
19	73.8, (d)	4.33, dd, 4.2, 4.0	42	70.0, (d)	4.90, dd, 2.1, 4.7	66	22.1, (q)	1.24, d, 7.0
20	73.6, (d)	4.11, dd, 4.0, 3.4	43	67.0, (d)	5.03, dd, 2.1, 9.0	67a	109.8, (t)	5.24, dd, 3.2
21	72.3, (d)	4.30, br d, 3.6	44	71.4, (d)	4.51, dd, 2.6, 8.7	67b		5.57, dd, 3.2
22	37.3, (t)	2.59, m	45	69.1, (d)	4.76, ddd, 2.6, 5.3, 9.3	68	21.4, (q)	0.89, d, 6.4
23	125.7, (d)	5.75, br d, 15.6	46a	41.5, (t)	2.11, br dd, 5.3, 12.9			
24	138.2, (d)	5.42, dd, 15.6, 7.7	46b		2.45, br dd, 8.8, 14.1			

<sup>a</sup> Protons on prochiral carbons are referred to as Ha for high fielded proton and Hb for low fielded proton.

MeOH, an HW-40 column with MeOH, and an ODS column with gradient elution from 50% to 100% aq MeOH. From 50 L of the harvested cells, 26 mg of **1** was isolated.

Compound **1** was isolated as a colorless amorphous solid:  $[\alpha]_{\text{D}}^{19} -19.2$  (c 0.10, H $_2$ O); IR (film) 3365, 1711  $\text{cm}^{-1}$ ; UV $_{\text{max}}$  ( $\lambda$ ) 231 ( $\epsilon$  44000), 260 ( $\epsilon$  38000), 270 ( $\epsilon$  47000), and 281 ( $\epsilon$  39000) nm. The high resolution ESI-TOF MS peak of **1** was observed at  $m/z$  1497.7074  $[\text{M} + \text{Na}]^+$ . This result indicated that a molecular formula was deduced to be C $_{68}$ H $_{114}$ O $_{34}$  ( $\Delta -1.5$  mmu).

The  $^{13}\text{C}$  NMR spectra were very complicated, and more than 68 carbon signals were observed when measured in methanol- $d_4$  or DMF- $d_7$  at room temperature. Signals around an acetal and a ketone carbon split into two or three signals, probably due to reversible formation of an acetal ring. To resolve this phenomenon, varieties of NMR measuring conditions such as solvents, temperature and pH were tested. Finally NMR measurements in pyridine- $d_5$ /D $_2$ O (6:1) at room temperature led simplified and improved the NMR spectra. Signals around the acetal and the ketone were observed as a single peak each in the  $^{13}\text{C}$  NMR spectrum. All carbon signals were assigned as 2 methyls, 12 aliphatic methylenes, 2 aliphatic methines, 1 oxymethylene, 33 oxymethines, 1 acetal, 16 olefinic carbons including 1 quaternary one, and 1 ketone (Table 1). UV absorption suggested the presence of diene and triene moieties similar to those of the amphidinols,<sup>2</sup> and these polyene structures were eventually confirmed by 2D NMR analyses.

Detailed analysis of ps (phase sensitive)-DQF COSY and TOCSY spectra led to elucidate four partial structures of **1**, H-1

to H-16, H-18 to H-34, H-36 to H-38, and H-40 to H-65 (Figure 1). HSQC-TOCSY experiments were useful to confirm proton connectivity around continuous oxymethines, H-1 to H-7, H-9 to H-14, and H-29 to H-32. Thus, four partial structures were constructed, and 68 carbons were assigned. These partial structures were interrupted by three quaternary carbons, the sp<sup>2</sup> quaternary carbon (C17,  $\delta_{\text{C}}$  155.6) bearing *exo*-methylene, the ketone (C35,  $\delta_{\text{C}}$  213.0) and the acetal (C39,  $\delta_{\text{C}}$  100.9) carbons. The HMBC correlations of H-67/C16, H-67/C17, H-67/C18, H-34/C35, H-36/C35, H-38/C39 and H-41/C39 measured in pyridine- $d_5$ /D $_2$ O (6:1) enabled us to trace all carbon connectivity. Unsaturation number and observed carbon signals corresponding to the ketone and eight double bonds indicated that **1** contained three rings in the molecule. The positions of these rings were deduced from deuterium shift experiments measured in pyridine- $d_5$ /H $_2$ O (6:1), and HMBC measurements. The deuterium shift experiments showed that five oxycarbons (C10, C14, C29, C32, and C43) were not shifted, so these carbons were involved in ether linkage. The HMBC correlations of H-43/C39 and H-10/C14 confirmed the six-membered rings. Therefore, the structure of **1** was determined as Figure 1 which has 30 hydroxy groups, 2 ether rings, 1 acetal ring, 1 ketone, and 8 double bonds on the C65-linear chain. Since **1** contains only 12 aliphatic methylenes in the molecule, **1** is relatively highly oxygenated to other linear carbon-chain compounds isolated from dinoflagellates.

Following the planar structural analysis, the conformation of the tetrahydropyran ring (C10 to C14) of **1** in the aqueous

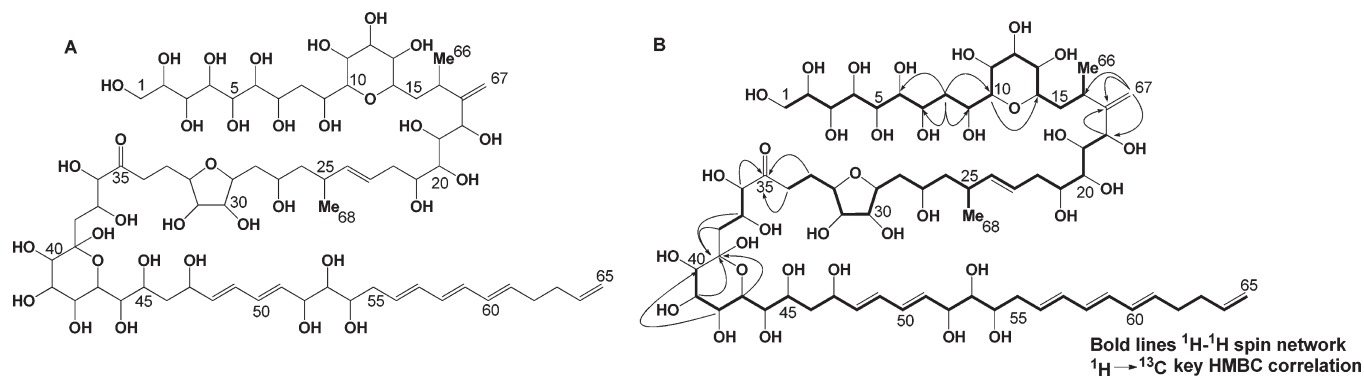


Figure 1. (A) Planar structure of **1**. (B)  $^1\text{H}$ – $^1\text{H}$  spin networks and HMBC correlations for **1**.

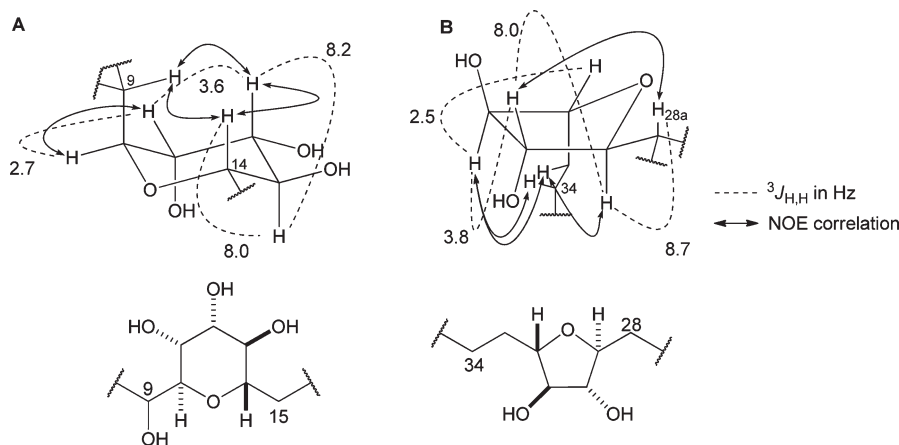


Figure 2. Relative stereoconfiguration of (A) C10 to C14 and (B) C29 to C32 of **1**.

pyridine solution was elucidated (Figure 2A). The observation of NOE correlations on H-9/H-12, H-9/H-14, H-12/H-14, and H-10/H-11 suggested that this ring forms a chair conformation with an axial orientation of C9. Furthermore, the small values of  $^3J_{\text{H-10,H-11}} = 2.7$  Hz,  $^3J_{\text{H-11,H-12}} = 3.6$  Hz indicated the equatorial orientation of H-10 and H-11. On the other hand, H-12, H-13, and H-14 were assigned as axial orientation from large coupling constants of  $^3J_{\text{H-12,H-13}} = 8.2$  Hz and  $^3J_{\text{H-13,H-14}} = 8.0$  Hz. Hence, vicinal coupling constants within this ring also supported that the C10 to C14 tetrahydropyran ring forms the chair conformation (Figure 2A). For the tetrahydrofuran ring (C29 to C32), the large vicinal coupling constants  $^3J_{\text{H-28a,H-29}} = 8.7$  Hz and  $^3J_{\text{H-29,H-30}} = 8.0$  Hz were indicative of anti orientation between both H-28a, H-29 and H-29, H-30, respectively. On the other hand, the magnitude of  $^3J_{\text{H-28b,H-29}} = 4.5$  Hz indicated that it was a value of gauche orientation for H-28b, H-29. From 2D NOESY spectra, NOE correlations on H-29/H-33, H-28a/H-30, H-31/H-33, and H-31/H-34 were observed; however, correlation signals heavily overlapped each other and further confirmation was required. Therefore, a part of **1** was subjected to reductive ozonolysis to solve the signal overlapping, and consequently a fragment corresponding to C24 to C48 was obtained. The conformation of this furan ring was identical between intact **1** and the ozonolyzed fragment, since the vicinal coupling constants pattern within this ring agreed well between both. From the 2D NOESY spectra of this fragment, the same NOE correlations as an intact **1** were observed. Hence, the relative configuration of protons on this ring was assigned as an  $\alpha$

direction for H-29 and H-31 and  $\beta$  for H-30 and H-32 as shown in Figure 2B. The conformation of the other cyclic moiety, a six-membered hemiacetal ring (C39 to C43), was also analyzed on the basis of ps-DQF COSY and 2D-NOESY spectra. The large magnitude of  $^3J_{\text{H-43,H-44}} = 9.0$  Hz indicated the anti orientation of H-43 to H-44; however, small coupling constants within this ring and lack of NOESY correlations hampered further configurational assignment.

Although the relative configuration of the above cyclic structures was analyzed by use of conventional NMR spectroscopic methods, the configurations of continuous polyol units on a long acyclic carbon chain were harder to determine. Therefore, the JBCA was applied for relative configurational analysis on them. For this purpose,  $^2,3J_{\text{C,H}}$  values, in addition to  $^3J_{\text{H,H}}$ , were obtained from HETLOC ( $\omega$ 1-hetero half-filtered TOCSY)<sup>28</sup> and HMBC<sup>29</sup> experiments (See Supporting Information).

The relative configurations of the longest polyol segment, a C1 to C9 portion, were analyzed by the JBCA (Figure 3). For the C2/C3 bond, large  $^3J_{\text{H-2,H-3}} = 8.2$  Hz and no NOE correlations on H-1/H-4 indicated the *erythro* configuration for C2 to C3. Small magnitude of vicinal proton coupling constant  $^3J_{\text{H-3,H-4}} = 2.2$  Hz was found for C3/C4 bond, which led the decrease of the relevant correlation peaks in HETLOC spectra except for  $^2J_{\text{C3,H-4}} = 1.1$  Hz. Each small value for  $^3J_{\text{C5,H-3}}$ ,  $^3J_{\text{C2,H-4}}$ , and  $^2J_{\text{C4,H-3}}$  obtained by the HMBC method indicated *threo* relationship of C3/C4. For the C4/C5 bond, a vicinal coupling constant  $^3J_{\text{H-4,H-5}} = 6.8$  Hz and small magnitude of  $^3J_{\text{C6,H-4}} = 2.4$  Hz were observed. On the other hand, large and medium magnitude of

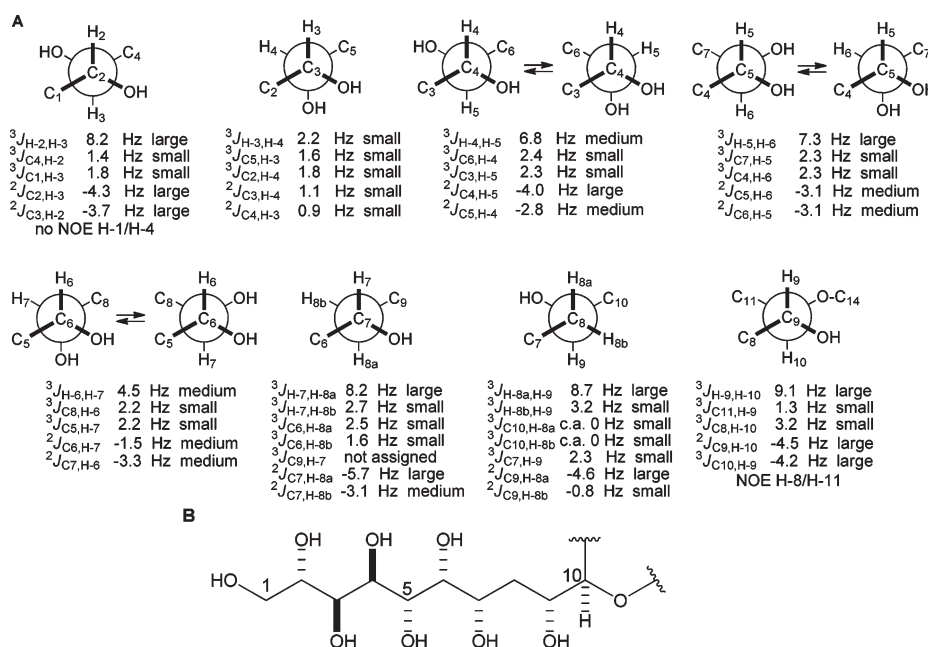


Figure 3. Relative configuration determined for the C1 to C9 part: (A) Newman projection, (B) structural diagram.

$^2J_{C4,H-5}$  and  $^2J_{C5,H-4}$  were indicative of the conformational exchange around C4/C5 bond with *erythro* configuration. For the C5/C6 bond, the observed vicinal coupling constant  $^3J_{H-5,H-6} = 7.3$  Hz corresponded to the border value between anti and gauche orientation. Otherwise, the medium long-range C–H coupling constants  $^2J_{C5,H-6} = -3.1$  Hz and  $^2J_{C6,H-5} = -3.1$  Hz were observed with the major C4/C7 gauche orientation. Hence a relative configuration was assigned to *threo* under conformational exchange. The moderate magnitude of vicinal coupling constant of  $^3J_{H-6,H-7} = 4.5$  Hz also suggested the presence of multiple alternating conformers. The observation of  $^3J_{C5,H-7} = 2.2$  Hz and  $^3J_{C8,H-6} = 2.2$  Hz indicated that both C5/H-7 and C8/H-6 were involved in gauche orientation. Thus the corresponding conformational mixture was deduced as Figure 3, where the relative configuration was determined as *threo* for the C6/C7 bond. The relative configuration between C7 and C9 mediated by C8 methylene was assignable by the JBCA. When the high and low fielded methylene protons were noted as H-8a and H-8b, respectively,  $^3J_{H-7,H-8a} = 8.2$  Hz, and  $^3J_{H-7,H-8b} = 2.7$  Hz were obtained from E. COSY cross sections. In addition to the vicinal proton coupling constants, the small magnitude of long-range C–H coupling constants  $^3J_{C6,H-8a} = 2.5$  Hz and  $^3J_{C6,H-8b} = 1.6$  Hz supported anti orientation of C6 to C9 and gauche orientations of C6 to H-8a and C6 to H-8b. In the same manner,  $^3J_{H-8a,H-9} = 8.7$  Hz,  $^3J_{H-8b,H-9} = 3.2$  Hz,  $^3J_{C10,H-8a} = \text{c.a. } 0$  Hz, and  $^3J_{C10,H-8b} = \text{c.a. } 0$  Hz were observed for C8 to C9, and these coupling constants supported the anti orientation of C7 to C10 and gauche orientation of C10 to H-8a and C10 to H-8b. Hence the orientation of C7-OH and C9-OH was assigned as syn. For the C9/C10 bond, the observation of large coupling constant  $^3J_{H-9,H-10} = 9.1$  Hz and NOESY correlations on H-8/H-11 indicated the *threo* configuration.

For the middle part of this molecule, a number of signals of HETLOC cross sections were too weak to detect presumably due to slow molecular motion in the measurement condition in addition to the high multiplicity of relevant proton signals. In order to overcome this problem for application of the JBCA,

relative signal intensities of ps-HMBC cross peaks ( $I_{C,H}$ ) were analyzed instead of long-range C–H coupling constants.<sup>30</sup> This approach shows the orientation of each atom by the relative magnitude of cross peak intensities and was applied to the C14 to C17 and C25 to C29 portions of 1.

For C15 to C16, small  $^3J_{H-15a,H-16} = 4.5$  Hz and large  $^3J_{H-15b,H-16} = 8.2$  Hz indicated gauche orientation between H-15a and H-16 and anti between H-15b and H-16. From F2 slice data of ps-HMBC spectra (Table 2), the signal intensities of  $I_{C17,H-15a}$  (65, large) and  $I_{C66,H-15a}$  (36, small) were obtained, and thus the relationships between C17 and H-15a, and C66 and H-15a were established to be anti and gauche, respectively. On the basis of these assignments, C66 and H-15b were determined to have gauche relationship automatically with the intensity of  $I_{C66,H-15b}$  (17, small). In the same manner, for a pyran ring adjacent C14 to C15 portion, large  $^3J_{H-14,H-15a} = 8.9$  Hz and small  $^3J_{H-14,H-15b} = 4.2$  Hz coupling constants were indicative of anti orientation between H-14 and H-15a, and gauche between H-14 and H-15b. Both the ps-HMBC signal intensities of C13/H-15b and C14/H-15b exhibited comparable magnitude in C66/H-15b. Therefore, the configuration of C13/H-15b, and C14-O/H-15b were assigned as gauche and anti relationships, respectively. Hence, the dominant conformation of C13 to C16 part was turned out to be zigzag, and the relationship between H-14 and C17 was established to be syn (Figure 4).

For C25 to C26, large  $^3J_{H-25,H-26a} = 8.7$  Hz and small  $^3J_{H-25,H-26b} = 4.7$  Hz were observed, suggesting gauche orientation between C24 and H-26a. Additionally, C24/H-26b and C68/H-26b correlations were large and small; the conformation between C24 and H-26b, and C68 and H-26b, were deduced to be anti and gauche, respectively. For the C26/C27 parts,  $^3J_{H-26a,H-27} = 3.6$  Hz and  $^3J_{H-26b,H-27} = 9.3$  Hz were observed, indicating the gauche orientation between C25 and H-27. Furthermore, the small magnitude of the cross peak for C28/H-26a suggested gauche orientation between C28 and H-26a. For the C27/C28 bond, small  $^3J_{H-27,H-28a} = 3.5$  Hz and large  $^3J_{H-27,H-28b} = 8.8$  Hz indicated gauche orientation between C29 and H-27. Since the small



Table 2. Signal Intensities of ps-HMBC Cross Peaks and Relevant C–H Orientation

<sup>1</sup> H	<sup>13</sup> C	<i>I</i> <sub>C,H</sub> <sup>*</sup>	magnitude	orientation		<sup>1</sup> H	<sup>13</sup> C	<i>I</i> <sub>C,H</sub> <sup>*</sup>	magnitude	orientation	
15a	13	9	small	H-15a/C13	gauche	26a	24	43	small	H26a/C24	gauche
	14	78	large	H-15a/C14-O	gauche		68	11	small	H26a/C68	gauche
	17	65	large	H-15a/C17	anti		27	13	small	H26a/C27-O	anti
	66	36	small	H-15a/C66	gauche		28	c.a. 1	small	H26a/C28	gauche
15b	13	17	small	H-15b/C13	gauche	26b	24	60	large	H26b/C24	anti
	14	8	small	H15b/C14-O	anti		68	17	small	H26b/C68	gauche
	17	35	small	H15b/C17	gauche		27	65	large	H26b/C27-O	gauche
	66	17	small	H-15b/C66	gauche		28	21	small	H26b/C28	gauche
						28a	26	<6	small	H28a/C26	gauche
							27	<8	small	H28a/C27-O	anti
							29	35	large	H28a/C29-O	gauche
						28b	26	13	small	H28b/C26	gauche
							27	55	large	H28b/C27-O	gauche
							29	19	small	H28b/C29-O	anti

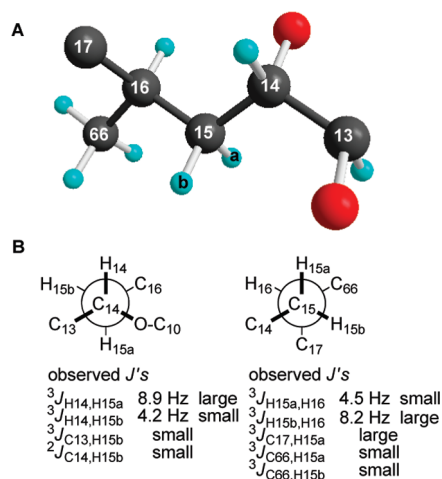


Figure 4. Relative configuration determined for C13 to C16: (A) schematic diagram, (B) Newman projections.

magnitude of the cross peak for C26/H-28a was found in the ps-HMBC spectrum, the relationship between C26 and H-28a was assigned as gauche orientation. For the C28/C29 bond, <sup>3</sup>J<sub>H-28a,H-29</sub> = 8.0 Hz and <sup>3</sup>J<sub>H-28b,H-29</sub> = 4.5 Hz indicated gauche orientation between C30 and H-28a. From the ps-HMBC spectrum, the magnitude of C29/H-28b cross peak was small. Thus, relationships between C29-O/H-28b, and between C29-O/H-28a were deduced to be anti and gauche orientation, respectively. Hence the configurational and conformational assignment for C25 to C29 moiety was achieved (Figure 5).

For the C52–C54 moiety, <sup>3</sup>J<sub>H-53,H-54</sub> = 7.2 Hz was obtained in ps-DQF COSY cross sections. In addition, NOE correlation of H-55/H-52 was not observed in 2D NOESY spectra measured at different temperatures (25, 0, and –10 °C). Therefore, the configuration between C53 and C54 was determined as *erythro*. In addition, the small coupling constant <sup>3</sup>J<sub>H-52,H-53</sub> = 3.2 Hz was obtained in ps-DQF COSY spectra. However, further observation of long-range C–H coupling constants through the C52/C53 bond was not successful even in the HMBC methods. Therefore, the Universal NMR database method developed by Kishi<sup>31</sup> was attempted to be applied for this system. In pyridine-*d*<sub>5</sub>, the coupling constants <sup>3</sup>J<sub>H-52,H-53</sub> = 2.7 Hz and <sup>3</sup>J<sub>H-53,H-54</sub> = 7.7 Hz

were obtained from the ps-DQF COSY spectrum, which were compared to the Universal NMR database for the triol system.<sup>31</sup> Resulted <sup>3</sup>J<sub>H,H</sub> assembly showed the best correspondence to the diastereomers of H-52/H-53 syn and H-53/H-54 anti out of four possible ones, being consistent with that deduced from JBCAs (Figure 6A). For the C18 to C21 tetraol unit, the JBCA was not helpful since the close chemical shift of H-19 (δ 4.33) and H-21 (δ 4.30) hampered accurate analyses of HETLOC and HMBC cross sections. In methanol-*d*<sub>4</sub>, <sup>3</sup>J<sub>H-18,H-19</sub> = 4.57 Hz, <sup>3</sup>J<sub>H-19,H-20</sub> = 4.18 Hz, and <sup>3</sup>J<sub>H-20,H-21</sub> = 4.47 Hz were obtained from the ps-DQF COSY spectrum, which were compared to the Universal NMR database (Figure 6B). Obtained <sup>3</sup>J<sub>H,H</sub> assembly indicated the configuration for C18 to C21 as shown in Figure 6B within the tolerable error level (Σ|ΔHz| < 2.5 Hz).<sup>32</sup> Thus the chemical structure of **1** was determined with a part of relative configurations as shown in Figure 7 by use of the best state of the art at the present.

This is the first isolation of the long carbon chain compound of a largely linear feature, from the genus *Prorocentrum*. The skeletal structure is reminiscent of amphidinols, although **1** does not exhibit potent hemolytic and antifungal activity exhibited by amphidinols. For the other bioactivity, **1** exhibited cytotoxicity against P388 cells at 16 μg/mL and antidiatom activity against *Nitzschia* sp. at 50 μg/mL. Interestingly, a weak interaction between prorocentrol and okadaic acid was suggested because proton NMR signals of okadaic acid shifted under the coexistence of prorocentrol. Investigations of the interaction, relative configuration on the C36–C47 part, and stereochemical correlations among C2–C16, C18–C21, C25–C29, C36–C47, and C52–C55 moieties are currently under way.

## EXPERIMENTAL SECTION

**NMR Measurement.** Chemical shift values are reported in ppm (δ) referenced to internal signals of residual protons [<sup>1</sup>H NMR; C<sub>5</sub>HD<sub>4</sub>N (δ 7.19), CHD<sub>2</sub>OD (δ 3.31); <sup>13</sup>C NMR; C<sub>5</sub>D<sub>3</sub>N (δ 123.5), CH<sub>3</sub>OD (δ 49.0)].

**Methods for Measuring <sup>2,3</sup>J<sub>C,H</sub>.** Long-range C–H coupling constants <sup>2,3</sup>J<sub>C,H</sub> were measured by using the following three methods: the HETLOC (*ω*1-hetero half-filtered TOCSY) with BIRD filter, ps (phase sensitive) HMBC, and *J*-HMBC.<sup>29</sup> For the HETLOC spectra, the MLEV-17 spin-lock periods were set for 30 or 60 ms. The *τ* interval

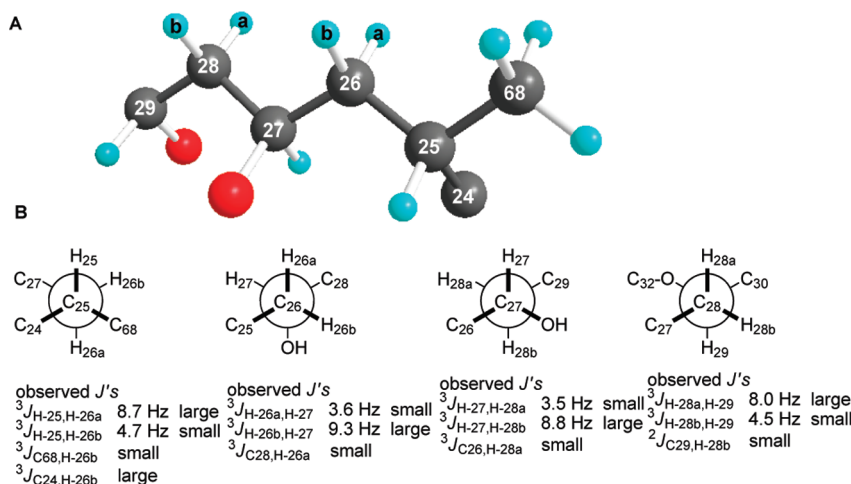


**Figure 5.** Relative configuration determined for C25 to C29: (A) schematic diagram, (B) Newman projections.

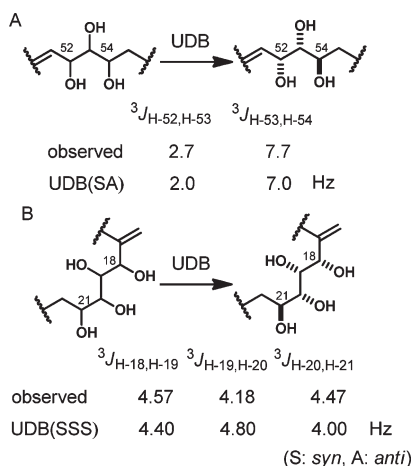


**Figure 6.** Relative configuration determined by Universal NMR database method: (A) for C52 to C54, (B) C18 to C21.

of BIRD filter was set for 500 ms in each experiment. The HETLOC spectra were acquired with 12 (for 60 ms mixing time) and 8 (for 30 ms mixing time) scans per increment for a  $4K (F_2) \times 512 (F_1)$  data matrix for the spectral width of 5600 Hz for both dimensions on an 800 MHz spectrometer at 25 °C. The HETLOC 2D-spectra were obtained through phase collection. The  $F_2$  slice 1D-spectra produced from the correlation peaks in 2D spectra were subjected to inverse Fourier translation to provide FIDs. These FIDs were processed with single exponential window before linear prediction processing to give the digital resolution of 0.34 Hz/pts. The ps-HMBC spectra were acquired with 40 scans per increment for a  $4K (F_2) \times 512 (F_1)$  data matrix for the spectral width of 3500 Hz ( $^1H$ ) and 26250 Hz ( $^{13}C$ ), respectively, with the delay set for 40 ms on a 500 MHz spectrometer at 25 °C. A linear prediction processing was conducted for both dimensions successive to a gauss window processing to give the digital resolution of 0.42 Hz/pts ( $F_2$ ) and 12.81 Hz/pts ( $F_1$ ), respectively. As another HMBC based method, a  $J$ -HMBC spectrum acquired with short  $^{2,3}J_{C,H}$  delay was also applied for the elucidation of  $^{2,3}J_{C,H}$  values. The  $J$ -HMBC cross peak intensities ( $I_{C,H}$ ) could be described in following relationship:  $I_{C,H} = |\sin(\pi^{2,3}J_{C,H}\Delta)|$ , where the  $\Delta$  means the  $^{2,3}J_{C,H}$  delay. In many cases, desired  $^{2,3}J_{C,H}$  was obtained from the least squared method by fitting a sine curve for the  $I_{C,H}$  depending on the characteristic  $\sin(\pi^{2,3}J_{C,H})$  with increasing the  $\Delta$ .<sup>29</sup> This method requires relatively long  $\Delta$  (200–500 ms).

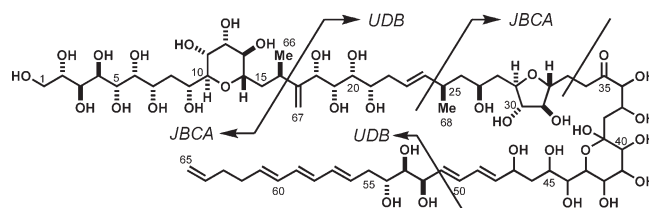


**Figure 7.** Partial relative configuration of 1. Stereochemical correlation of each segment is not elucidated.

However for procontrol, decrease in  $J$ -HMBC cross peak intensities was observed even in 200 ms of  $\Delta$ . Therefore the proportional ratio of  $^{2,3}J_{C,H}$  and cross peak intensities were applied for  $^{2,3}J_{C,H}$  analysis along following relationship:  $I_{C_a, H_a} / |\sin(\pi^{2,3}J_{C_a, H_a}\Delta)| = I_{C_b, H_a} / |\sin(\pi^{2,3}J_{C_b, H_a}\Delta)|$ . The  $J$ -HMBC spectrum was measured with 94 scans per increment for a  $2K (F_2) \times 1K (F_1)$  data matrix for the spectral width of 3000 Hz ( $^1H$ ) and 31250 Hz ( $^{13}C$ ), respectively, with the delay set for 50 ms on a 500 MHz spectrometer at 25 °C. Two-fold zero filling for the  $F_2$  dimension and linear prediction processing was conducted for the  $F_1$  dimension successive to sine bell window processing to give the digital resolution of 0.73 Hz/pts ( $F_2$ ) and 7.62 Hz/pts ( $F_1$ ), respectively.

**Microalgal Material.** A clonal culture of the dinoflagellate *Procentrum hoffmannianum* Faust (CCMP683)<sup>17</sup> was obtained from the Provasoli-Guillard National Center for Culture of Marine Phytoplankton, which was originally isolated at Florida, USA. Laboratory cultures of *P. hoffmannianum* were performed in 3 L fernbach flasks containing f/2 supplement at 25 °C under irradiation of 40 W white fluorescent lamps at 39–46  $\mu\text{mol m}^{-2}\text{s}^{-1}$  for 18/6 h light/dark photocycle for 30–45 days.

**Isolation and Purification of 1.** The harvested cells from 50 L of culture media were extracted with MeOH (400 mL  $\times$  3) and acetone (400 mL  $\times$  3). The combined extract was concentrated in vacuo, and the resulted residue was suspended in 500 mL of water and partitioned with 200 mL of hexane 3 times and then 200 mL of ethyl acetate 4 times. From the aqueous layer, compound 1 was extracted 6 times with 300 mL of *n*-butanol each. The obtained *n*-butanol layer was concentrated in vacuo and partitioned between 15 mL of 0.15% v/v aqueous acetic acid and ethyl acetate to remove residual okadaic acid. The aqueous acetic acid layer was applied on an ODS column and eluted with 80% MeOH (50 mL) and 100% MeOH (100 mL), sequentially. The 80% MeOH eluent was applied on a GPC column and eluted with MeOH at a flow rate of 2 mL/min to afford crude 1 ( $t_R$  26–47 min). Concentrated

fraction was purified using ODS MPLC with gradient elution of 50% MeOH for 12 min, 50% to 100% MeOH for 24 min, and 100% MeOH for 24 min sequentially at a flow rate of 5 mL/min to furnish **1** (26 mg,  $t_R$  25–30 min).

**Prorocentrol (1).** Isolated as a colorless amorphous solid:  $[\alpha]_D^{19} -19.2$  ( $c$  0.10, H<sub>2</sub>O); IR (film) 3365, 1711 cm<sup>-1</sup>; UV<sub>max</sub> ( $\lambda$ ) 231 ( $\epsilon$  44000), 260 ( $\epsilon$  38000), 270 ( $\epsilon$  47000), and 281 ( $\epsilon$  39000) nm. The high resolution ESI-TOF MS of **1** gave  $[M + Na]^+$  at  $m/z$  1497.7074, corresponding to a molecular formula of C<sub>68</sub>H<sub>114</sub>O<sub>34</sub> ( $\Delta\delta$  -1.5 mmu) for **1**. Assignment of <sup>1</sup>H and <sup>13</sup>C NMR signals are noted in Table 1.

**Cytotoxicity Assay.** Cytotoxicity of **1** against P388 murine leukemia cells was measured by using a MTT colorimetric method. After adding the sample solution to a 96-well microplate, P388 cells were inoculated to a density of 500 cells/well. After 96 h of incubation at 37 °C, 50  $\mu$ L of 1.0 mg/mL aqueous MTT (3-(4,5-dimethylthiazol-2-yl)-2,5-diphenyltetrazolium bromide) was added to the sample solution and incubated for another 4 h under the same condition. Then the supernatant was removed by aspiration. The remained precipitation was dissolved in 100  $\mu$ L of DMSO, and absorbance was measured at 570 nm.

**Antidiatom Assay.** *Nitzschia* sp. was cultured in natural seawater supplemented by ES-1<sup>17</sup> nutrient in the same way as *P. hoffmannianum*. In a 24-well microplate were placed 250  $\mu$ L of *Nitzschia* sp. incubated to a steady state, 750  $\mu$ L of fresh media, and **1** in 5  $\mu$ L of DMSO. After 1 day of incubation, antidiatom activity of **1** against *Nitzschia* sp. was evaluated by visual counting.

**Ozonolysis of 1.** Ozone gas was bubbled through a solution of **1** (16.6 mg) in 5 mL of H<sub>2</sub>O at 0 °C until excessive ozone was observed. To this solution was added NaBH<sub>4</sub> (10 mg, 0.27 mmol) suspended in MeOH, and the mixture was allowed to stand at ambient temperature for 10 h. To the reaction mixture was added acetic acid to quench the reaction. After removal of the solvent, obtained solid was dissolved in H<sub>2</sub>O and purified by using ODS HPLC column with 5%, 30%, 70% MeOH, and MeOH stepwise gradient elution to afford a pure fragment (500  $\mu$ g,  $t_R$  7–20 min in 5%) as a colorless solid. The high resolution ESI-TOF MS of the fragment gave  $[M + Na]^+$  at  $m/z$  657.2940. <sup>1</sup>H NMR (500 MHz, pyridine-*d*<sub>5</sub>/D<sub>2</sub>O (6:1))  $\delta$ : 3.60 (dd,  $J$  = 6.6, 11.0 Hz, H-24'a), 3.68 (dd,  $J$  = 5.3, 10.3 Hz, H-24'b), 2.08 (m, H-25'), 1.57 (ddd,  $J$  = 5.9, 7.3, 14.1 Hz, H-26a'), 1.69 (ddd,  $J$  = 7.3, 5.1, 13.3 Hz, H-26b'), 4.25 (dddd,  $J$  = 5.1, 7.3, 2.9, 9.5 Hz, H-27'), 1.86 (ddd,  $J$  = 2.9, 8.8, 13.2 Hz, H-28a'), 2.00 (ddd,  $J$  = 3.7, 9.5, 14.1 Hz, H-28b'), 4.63 (ddd,  $J$  = 3.8, 8.9, 8.9 Hz, H-29'), 4.18 (dd,  $J$  = 3.8, 8.1 Hz, H-30'), 4.35 (dd,  $J$  = 2.9, 5.1 Hz, H-31'), 4.40 (ddd, 2.5, 2.5, 10.3 Hz, H-32'), 2.43 (ddd,  $J$  = 2.9, 8.8, 15.0 Hz, H-33a'), 2.83 (ddd,  $J$  = 2.2, 10.0, 17.6 Hz, H-33b'), 2.49 (ddd,  $J$  = 2.6, 2.6, 8.8 Hz, H-34'), 4.60 (dd,  $J$  = 2.6, 2.6 Hz, H-35'), 3.85 (dd,  $J$  = 2.6, 9.7 Hz, H-36'), 4.70 (dd,  $J$  = 5.1, 9.5, 10.5 Hz, H-37'), 2.30 (dd,  $J$  = 11.7, 13.9 Hz, H-38a'), 2.78 (dd,  $J$  = 5.1, 14.0 Hz, H-38b'), 4.59 (d,  $J$  = 8.7 Hz, H-40'), 4.49 (dd,  $J$  = 9.1, 1.5 Hz, H-41'), 4.89 (dd,  $J$  = 1.8, 1.8 Hz, H-42'), 4.54 (dd,  $J$  = 1.6, 8.6 Hz, H-43'), 4.29 (dd,  $J$  = 2.2, 8.8 Hz, H-44'), 4.80 (ddd,  $J$  = 8.7, 5.1, 2.1 Hz, H-45'), 2.26 (ddd,  $J$  = 5.1, 5.1, 14.7 Hz, H-46a'), 2.32 (ddd,  $J$  = 8.6, 8.6, 14.7 Hz, H-46b'), 4.40 (m, H-47'), 3.89 (d,  $J$  = 5.4 Hz, H-48'), 1.00 (d,  $J$  = 6.6 Hz, H-68'); <sup>13</sup>C NMR (100 MHz, pyridine-*d*<sub>5</sub>/D<sub>2</sub>O (6:1))  $\delta$ : 66.8 (C24', CH<sub>2</sub>), 32.6 (C25', CH), 42.3 (C26', CH<sub>2</sub>), 66.6 (C27', CH), 42.1 (C28', CH<sub>2</sub>), 78.5 (C29', CH), 78.1 (C30', CH), 73.4 (C31', CH), 73.6 (C32', CH), 25.1 (C33', CH<sub>2</sub>), 39.5 (C34', CH<sub>2</sub>), 68.7 (C35', CH), 78.0 (C36', CH), 67.7 (C24', CH), 38.5 (C38', CH<sub>2</sub>), 68.9 (C40', CH), 76.7 (C41', CH), 68.9 (C42', CH), 74.9 (C43', CH), 73.0 (C44', CH), 69.0 (C45', CH), 37.8 (C46', CH<sub>2</sub>), 71.2 (C47', CH), 66.6 (C48', CH<sub>2</sub>), 17.8 (C68', CH<sub>3</sub>). The signal of C39' was not observed probably because of the limited amount.

## ■ ASSOCIATED CONTENT

Supporting Information. <sup>1</sup>H, <sup>13</sup>C, ps-DQF COSY, E. COSY, NOESY, <sup>13</sup>C–<sup>1</sup>H COSY, HSQC-TOCSY, HMBC, ps-

HMBC, J-HMBC and HETLOC spectra of **1**. This material is available free of charge via the Internet at <http://pubs.acs.org>.

## ■ AUTHOR INFORMATION

### Corresponding Author

\*E-mail: [msatake@chem.s.u-tokyo.ac.jp](mailto:msatake@chem.s.u-tokyo.ac.jp); [ktachi@chem.s.u-tokyo.ac.jp](mailto:ktachi@chem.s.u-tokyo.ac.jp).

### Present Addresses

<sup>†</sup>Department of Chemistry, Graduate School of Science, Osaka University, Machikaneyama, Toyonaka, Osaka 560-0043, Japan.

## ■ ACKNOWLEDGMENT

The authors are grateful to Dr. Ryan van Wagoner at the University of North Carolina, Wilmington for critical reading of the manuscript. This work was supported by KAKENHI (22404006), Global COE Program for Chemistry Innovation, the University of Tokyo, and The Circle for the promotion of science and Engineering. The authors also thank Drs. Yu Tsutsumi (JEOL Ltd.), Chisato Kurosaki, and Mayumi Yoshida (Yokohama Institute, RIKEN) for performing the NMR experiments.

## ■ REFERENCES

- (1) Murata, M.; Yasumoto, T. *Chem. Rev.* **1993**, *93*, 1897–1909.
- (2) (a) Satake, M.; Murata, M.; Yasumoto, T.; Fujita, T.; Naoki, H. *J. Am. Chem. Soc.* **1991**, *113*, 9859–9861. (b) Paul, G. K.; Matsumori, N.; Murata, M.; Tachibana, K. *Tetrahedron Lett.* **1995**, *36*, 6279–6282. (c) Paul, G. K.; Matsumori, N.; Konoki, K.; Murata, M.; Tachibana, K. *J. Mar. Biotechnol.* **1997**, *5*, 124–128. (d) Echigoya, R.; Rhodes, L.; Oshima, Y.; Satake, M. *Harmful Algae* **2005**, *4*, 383–389. (e) Morsy, M.; Matsuoka, S.; Houdai, T.; Matsumori, N.; Adachi, S.; Murata, M.; Iwashita, T.; Fujita, T. *Tetrahedron* **2005**, *61*, 8606–8610.
- (3) (a) Doi, Y.; Ishibashi, M.; Nakamichi, H.; Kosaka, T.; Ishikawa, T.; Kobayashi, J. *J. Org. Chem.* **1997**, *62*, 3820–3823. (b) Kubota, T.; Tsuda, M.; Doi, Y.; Takahashi, A.; Nakamichi, H.; Ishibashi, M.; Fukushima, E.; Kawabata, J.; Kobayashi, J. *Tetrahedron* **1998**, *54*, 14455–14464. (c) Kubota, T.; Takahashi, A.; Tsuda, M.; Kobayashi, J. *Mar. Drugs* **2005**, *3*, 113–118.
- (4) (a) Huang, X.; Zhao, D.; Guo, Y.; Wu, H.; Lin, L.; Wang, Z.; Ding, J.; Lin, Y. *Bioorg. Med. Chem. Lett.* **2004**, *14*, 3117–3120. (b) Huang, X.; Zhao, D.; Guo, Y.; Wu, H.; Trivellone, E.; Cimino, G. *Tetrahedron Lett.* **2004**, *45*, 5501–5504.
- (5) Washida, K.; Koyama, T.; Yamada, K.; Kita, M.; Uemura, D. *Tetrahedron Lett.* **2006**, *47*, 2521–2525.
- (6) (a) Kobayashi, J.; Kubota, T.; Takahashi, M.; Ishibashi, M.; Tsuda, M.; Naoki, H. *J. Org. Chem.* **1999**, *64*, 1478–1482. (b) Kubota, T.; Tsuda, M.; Takahashi, M.; Ishibashi, M.; Naoki, H.; Kobayashi, J. *J. Chem. Soc., Perkin Trans. 1* **1999**, *64*, 3483–3487. (c) Kubota, T.; Tsuda, M.; Takahashi, M.; Ishibashi, M.; Oka, S.; Kobayashi, J. *Chem. Pharm. Bull.* **2000**, *48*, 1447–1451.
- (7) Kubota, T.; Sakuma, Y.; Shimbo, K.; Tsuda, M.; Nakano, M.; Uozumi, Y.; Kobayashi, J. *Tetrahedron Lett.* **2006**, *47*, 4369–4371.
- (8) (a) Usami, M.; Satake, M.; Ishida, S.; Inoue, A.; Kan, Y.; Yasumoto, T. *J. Am. Chem. Soc.* **1995**, *117*, 5389–5390. (b) Ukena, T.; Satake, M.; Usami, M.; Oshima, Y.; Naoki, H.; Fujita, T.; Kan, Y.; Yasumoto, T. *Biosci. Biotechnol. Biochem.* **2001**, *65*, 2585–2588. (c) Ukena, T.; Satake, M.; Usami, M.; Oshima, Y.; Fujita, T.; Naoki, H.; Yasumoto, T. *Rapid Commun. Mass Spectrom.* **2002**, *16*, 2387–2397.
- (9) Kita, M.; Roy, M. C.; Siwu, E. R. O.; Noma, I.; Takiguchi, T.; Itoh, M.; Yamada, M.; Koyama, T.; Iwashita, T.; Uemura, D. *Tetrahedron Lett.* **2007**, *48*, 3423–3427.
- (10) Tsunematsu, Y.; Ohno, O.; Konishi, K.; Yamada, K.; Suganuma, M.; Uemura, D. *Org. Lett.* **2009**, *11*, 2153–2156.



- (11) (a) Wagoner, R. M. V.; Deeds, J. R.; Satake, M.; Ribeiro, A. A.; Place, A. R.; Wright, J. L. C. *Tetrahedron Lett.* **2008**, 49, 6457–6461. (b) Wagoner, R. M. V.; Deeds, J. R.; Tatters, A. O.; Place, A. R.; Tomas, C. R.; Wright, J. L. C. *J. Nat. Prod.* **2010**, 73, 1360–1365.
- (12) (a) Houdai, T.; Matsuoka, S.; Morsy, N.; Matsumori, N.; Satake, M.; Murata, M. *Tetrahedron* **2005**, 61, 2795–2802. (b) Inuzuka, T.; Uemura, D.; Arimoto, H. *Tetrahedron* **2008**, 64, 7718–7723.
- (13) (a) Torigoe, K.; Murata, M.; Yasumoto, T.; Iwashita, T. *J. Am. Chem. Soc.* **1988**, 110, 7876–7877. (b) Hu, T.; deFreitas, A. S.; Curtis, J. M.; Oshima, Y.; Walter, J. A.; Wright, J. L. C. *J. Nat. Prod.* **1996**, 59, 1010–1014.
- (14) Lu, C. K.; Lee, G. H.; Huang, R.; Chou, H. N. *Tetrahedron Lett.* **2001**, 42, 1713–1716.
- (15) Hu, T.; Curtis, J. M.; Walter, J. A.; Wright, J. L. C. *Tetrahedron Lett.* **1999**, 40, 3977–3980.
- (16) Lu, C. K.; Chou, H. N.; Lee, C. K.; Lee, T. H. *Org. Lett.* **2005**, 7, 3893–3896.
- (17) Culture and collection information are referred from the database of Provasoli-Guillard National Center for Culture of Marine Phytoplankton. Homepage: <https://ccmp.bigelow.org/>
- (18) Matsumori, N.; Kaneno, D.; Murata, M.; Nakamura, H.; Tachibana, K. *J. Org. Chem.* **1999**, 64, 866–876.
- (19) Murata, M.; Matsuoka, S.; Matsumori, N.; Tachibana, K. *J. Am. Chem. Soc.* **1999**, 121, 870–871.
- (20) (a) Nonomura, T.; Sasaki, M.; Matsumori, N.; Murata, M.; Tachibana, K.; Yasumoto, T. *Angew. Chem., Int. Ed.* **1996**, 35, 1675–1678. (b) Sasaki, M.; Matsumori, N.; Maruyama, T.; Nonomura, T.; Murata, M.; Tachibana, K.; Yasumoto, T. *Angew. Chem., Int. Ed.* **1996**, 35, 1672–1675.
- (21) Peng, J.; Place, A. R.; Yoshida, W.; Anklin, C.; Hamann, M. T. *J. Am. Chem. Soc.* **2010**, 132, 3277–3279.
- (22) Hanif, H.; Ohno, O.; Kitamura, M.; Yamada, K.; Uemura, D. *J. Nat. Prod.* **2010**, 73, 1318–1322.
- (23) Napolitano, J. G.; Norte, M.; Padrón, J. M.; Fernández, J. J.; Hernández, D. A. *Angew. Chem., Int. Ed.* **2009**, 48, 796–799.
- (24) (a) Bedke, D. K.; Shibuya, G. M.; Pereira, A.; Gerwick, W. H.; Haines, T. H.; Vanderwal, C. D. *J. Am. Chem. Soc.* **2009**, 131, 7570–7572. (b) Kawahara, T.; Kumaki, Y.; Kamada, T.; Ishii, T.; Okino, T. *J. Org. Chem.* **2009**, 74, 6016–6024.
- (25) Park, H. R.; Chijiwa, S.; Furihata, K.; Hayakawa, Y.; Shin-ya, K. *Org. Lett.* **2007**, 9, 1457–1460.
- (26) Nagatsu, A.; Tanaka, R.; Mizukami, H.; Ogihara, Y.; Sakakibara, J. *Tetrahedron* **2001**, 57, 3369–3372.
- (27) Matsumori, N.; Murata, M.; Tachibana, K. *Tetrahedron* **1995**, 51, 12229–12238.
- (28) Wollborn, U.; Leibfritz, D. *J. Magn. Reson.* **1992**, 98, 142–146.
- (29) (a) Willker, W.; Leibfritz, D. *Magn. Reson. Chem.* **1995**, 33, 632–638. (b) Biesemans, M.; Martins, J. C.; Willem, R.; Lyčka, A.; Růžicka, A.; Holeček, J. *Magn. Reson. Chem.* **2002**, 40, 65–69. (c) Takayama, H.; Ichikawa, T.; Kuwajima, T.; Kitajima, M.; Seki, H.; Aimi, N.; Nonato, M. G. *J. Am. Chem. Soc.* **2000**, 122, 8635–8639. (d) Seki, H.; Tokunaga, T.; Utsumi, H.; Yamaguchi, K. *Tetrahedron* **2000**, 56, 2935–2939. (e) Iida-Tanaka, N.; Fukase, K.; Utsumi, H.; Ishizuka, I. *Eur. J. Biochem.* **2000**, 267, 6790–6797.
- (30) (a) Sakai, R.; Kamiya, H.; Murata, M.; Shimamoto, K. *J. Am. Chem. Soc.* **1997**, 119, 4112–4116. (b) Zhu, G.; Bax, A. *J. Magn. Reson.* **1993**, 98, 142–146. (c) Marquez, B. L.; Gerwick, W. H.; Williamson, R. T. *Magn. Reson. Chem.* **2001**, 39, 499–530.
- (31) Higabayashi, S.; Czechtizky, W.; Kobayashi, Y.; Kishi, Y. *J. Am. Chem. Soc.* **2003**, 125, 14379–14393.
- (32) Seike, H.; Ghosh, I.; Kishi, Y. *Org. Lett.* **2006**, 8, 3861–3864.

## NOTE ADDED AFTER ASAP PUBLICATION

Figure 7 was incorrect in the version published ASAP March 22, 2011. The correct version reposted March 30, 2011.